Journal of Fluorescence, Vol. 10, No. 4, 2000

Molecular Dynamics of Biological Probes by Fluorescence Correlation Microscopy with Two-Photon Excitation

E. Guiot,[1,5] M. Enescu,[2] B. Arrio,[3] G. Johannin,[3] G. Roger,[1] S. Tosti,[4] F. Tfibel,[2] F. Mérola,[4] A. Brun,[1] P. Georges,[1] and M. P. Fontaine-Aupart[2]

Received November 1, 1999; revised June 21, 2000; accepted June 23, 2000

We report on the application of fluorescence correlation microscopy under two-photon excitation of fluorophores of biological interest: FITC–dextran (MW, from 20 to 150 kDa), green fluorescent protein (MW, 27 kDa), and fluorescein (MW, 330 Da). Under these experimental conditions, the translational diffusion coefficients of these molecules in aqueous solutions derived from the fluorescence intensity autocorrelation function were determined for the first time and were found to be 24×10^{-7}, 8.2×10^{-7}, and 3×10^{-7} cm^2 s^{-1} for 150-kDa FITC–dextran, green fluorescent protein, and fluorescein, respectively. These results are discussed in connection with previously reported results obtained by different methods. The great sensibility of the system has been applied to single-molecule detection of the smaller fluorophore, fluorescein.

KEY WORDS: Two-photon excitation; fluorescence correlation microscopy; translational diffusion; single-molecule detection.

INTRODUCTION

Fluorescence correlation spectroscopy (FCS) was proposed as a probe of molecular dynamics many years ago [1–3]. It is based on the analysis of temporal fluctuations of fluorescence intensity emerging from a very small volume containing few fluorescent molecules. In this way, information concerning the absolute number of fluorescent molecules in the excitation volume, diffusion coefficients, and rate constants of chemical reactions can be obtained. The application domain of FCS is continuously increasing, especially in the study of motion in biological environments where low molecular concentrations are confined in small volumes [4–6].

Among the experimental difficulties associated with FCS, one is the excitation confinement. This problem has been successfully solved by using the confocal microscopy technique [7–9] or the two-photon excitation (TPE) method [10–12]. By combining FCS and microscopy techniques, probing volume elements of about 1 fL has become possible. This technique has recently received the name of fluorescence correlation microscopy (FCM) [5].

There are some benefits in associating FCM with the two-photon excitation method: the excitation volume is intrinsically confined, the scattered excitation radiation can be easily rejected by means of spectral filtering, the eventual sample damage is restricted to the excitation volume, and the best penetration depth for thick biological sample can be obtained. Consequently, very low background production is possible in TPE experiments and this allows single-molecule detection [11,13]. Generally fluorescence emission properties for confocal and two-photon excitation techniques are similar as far as they

[1] Laboratoire Charles Fabry de l'Institut d'Optique, UMR 8501, 91403 Orsay Cedex, France.
[2] Laboratoire de Photophysique Moléculaire, UPR 3361, Faculté des Sciences, 91405 Orsay Cedex, France.
[3] Laboratoire de Bioénergie Membranaire, 91405 Orsay Cedex, France.
[4] Laboratoire pour l'Utilisation du Rayonnement Electromagnétique, 91898 Orsay Cedex, France.
[5] To whom correspondence should be addressed. e-mail: elvire.guiot@iota.u-psud.fr

1053-0509/00/1200-0413$18.00/0

are limited by fluorescence saturation processes [13]. Because of its strong dependence on the photophysics of the molecule under study, the extension of FCM application to different molecular species requires a particular analysis of parameters such as excitation saturation level, nonfluorescent state formation, and two-photon absorption probabilities.

In this study, FCM with TPE is, for the first time to our knowledge, used to determine the diffusion coefficient of representative probes commonly selected as *in vivo* probes: FITC–dextran of molecular weights ranging from 20 to 150 kDa, green fluorescent protein (GFP), and fluorescein. Correlation fluorescence of single molecules was an attempt to show the sensibility of the method.

MATERIALS AND METHODS

Experimental Setup

The fluorescence excitation source is a femtosecond Ti:sapphire laser (Coherent; MIRA 900) pumped in the green by a cw diode-pumped solid-state laser (Coherent; VERDI) (Fig. 1). The femtosecond laser produces 100-fs pulses in the near-IR (690–990 nm) at a repetition rate of 76 MHz. The present measurements were performed at 800 nm. The laser beam enters through the rear port of a modified Zeiss Axiovert 135 microscope and is focused on the sample with a Zeiss oil immersion objective (63×; NA = 1.4). To keep the pulse duration at 100 fs at the focus of the objective, a sequence of prisms is used to compensate the positive group velocity dispersion. The fluorescence is collected by the same objective, separated from the excitation radiation by a dichroic, mirror and detected by a photomultiplier tube (Hamamatsu, R7205-01). The residual laser radiation is removed by a set of interference filters placed in front of the photomultiplier. The photomultiplier is connected to an amplifier and timing discriminator (EG&G Ortec 9327) which provides TTL pulses. These pulses are sent to an acquisition card (National Instrument; DAQ PCI-6602) which is used in the buffer event counting mode. They are counted during a temporal gate which is typically in the range of a microsecond. After collection, data are transferred to a personal computer (500 MHz) and analyzed by homemade programs.

Fluorescent Probes

Fluorescent beads of 28-nm diameter were obtained from Molecular Probes and used in suspension in distilled water. Solutions were sonicated and filtered before each experiment. FITC–dextran (fluorescein isothiocyanate–dextran) of molecular mass ranging from 20 to 150 kDa (Sigma) was prepared in 5 m*M* HEPES buffer, pH 7.5, and centrifugated for 45 min at 100,000 *g* to eliminate aggregates. Fluorescein (Sigma) was prepared in the same buffer. Recombinant green fluorescent protein (rGFP), recombinant GFPuv (rGFPuv), and recombinant EGFP (rEGFP) from Clontech were solved in 5 m*M* Tris buffer, pH 8.

All assayed solutions were freshly prepared to avoid bacterial contamination and product degradation.

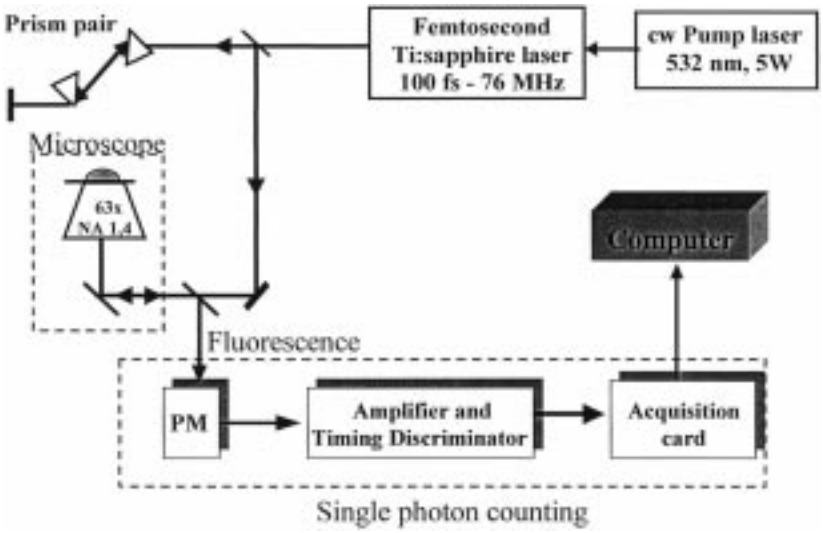

Fig. 1. Experimental setup for two-photon excitation fluorescence correlation microscopy.

Measurement and Analysis of Fluorescence Intensity Autocorrelation Functions

The digital photocount autocorrelation is defined as [14]

$$G(\tau) = N_c^{-1} \sum_{i=1}^{N_c} n(iT)n(iT + \tau) \quad (1)$$

where T is the period of counting intervals, N_c is the number of counting intervals, $n(iT)$ is the number of photons detected in the ith time interval, and τ is a multiple of T.

The detection system provides at each moment the number of photons detected from the start of the acquisition process. The vector $n(iT)$ is then processed to calculate the autocorrelation function for different delay times.

Usually, the excitation intensity distribution can be approximated by a three-dimensional Gaussian distribution [8,13]:

$$I(x, y, z) = \exp(-2(x^2 + y^2)/\omega_0^2) \exp(-2z^2/z_0^2) \quad (2)$$

where ω_0 is the beam waist at the focal point and z_0 the focal depth.

For this profile, the normalized autocorrelation function of the fluorescence intensity of diffusing particles is [2,5,8,9]

$$g(\tau) = 1 + \frac{(1 - I_b/S)^2}{\sqrt{8}N} \left(1 + \frac{Fe^{-\tau/\tau_r}}{1 - F}\right)\left(\frac{1}{1 + (\tau/\tau_d)}\right)\left(\frac{1}{1 + (\omega_0/z_0)^2 (\tau/\tau_d)}\right)^{1/2} \quad (3)$$

Experimental curves are fitted by a least-squares program based on the conjugated gradient method to obtain the number N of fluorescent molecules in the excitation volume, the ratio ω_0/z_0, and the translational diffusion time τ_d. The ratio of the background intensity I_b to the total signal intensity S is included to correct the decrease in the amplitude caused by the background signal. The exponential term takes into account the formation of the reversible nonfluorescent state (in particular, the triplet state), with F representing the fraction of molecules in this state and τ_T its lifetime.

In the case of TPE, the translational diffusion coefficient D is then calculated as [13,15]

$$D = \omega_0^2/8\tau_d \quad (4)$$

RESULTS AND DISCUSSION

Power-Squared Dependence and Saturation of Two-Photon Excited Fluorescence

For two-photon excitation, the dependence of the fluorescence intensity with respect to the incident intensity must be quadratic when the number of absorbing molecules is not significantly affected by the irradiation. Indeed, at a high excitation intensity, deviation from this square law can occur because of different processes such as excited-state absorption, excited-state saturation, accumulation of the molecules in the triplet state, and background contributions [16,17].

The quadratic dependence for FITC–dextran, rGFP, and fluorescein is presented in Figs. 2a, b, and c, respectively. Here, the fluorescence counting rate is studied as a function of the photon flux in the excitation volume. In the case of a spatially and temporally Gaussian laser beam, this photon flux in the focal plane is expressed as

$$N(r, t) = N_0 \exp(-2r^2/\omega_0^2) \exp(-t^2/\tau^2) \quad (5)$$

where N_0 represents the maximum photon flux during the laser pulse and τ is the duration of the laser pulse.

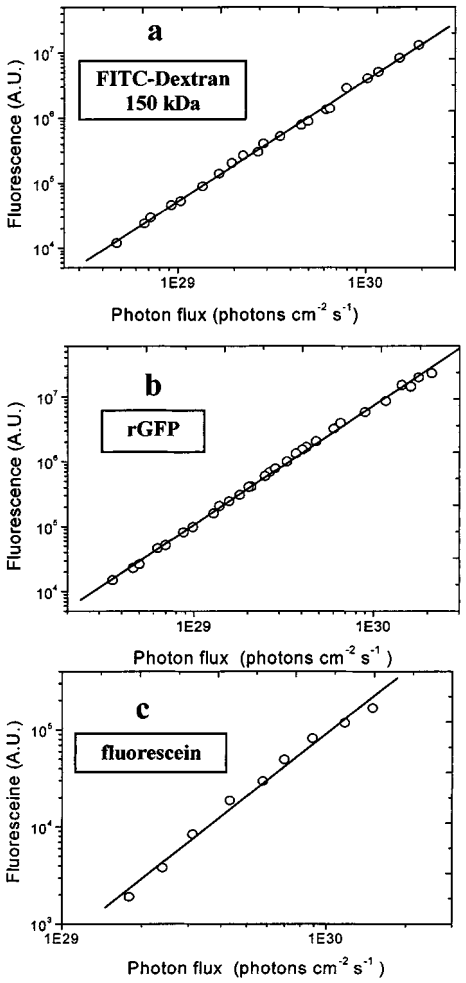

Fig. 2. Fluorescence counting rate versus photon flux incident on the sample: (a) 150-kDa FITC–dextran, 100 n*M*, in 5 m*M* HEPES buffer, pH 7.5; (b) rGFP, 400 n*M*, in 5 m*M* Tris buffer, pH 8; (c) fluorescein, 100 n*M*, in 5 m*M* HEPES buffer, pH 7.5.

N_0 is calculated from the laser power P incident on the sample:

$$N_0 = \frac{2}{\pi^{3/2}} \frac{P}{f} \frac{1}{\tau\omega_0^2} \frac{1}{h\nu} \quad (6)$$

Here, f is the laser repetition rate an $h\nu$ is the photon energy.

No significant deviation from square-law dependence is observed over the whole energy range of our laser (corresponding to a maximum average power of 100 mW at the focusing point of objective) for the three molecular species.

Calibration of the Excitation Volume

To calibrate the excitation volume, fluorescence correlation measurements were performed on known size particles which can be assumed to be spherical: latex beads and FITC–dextran. These entities, often used in biological experiments, have the advantage that each particle or molecule contains several fluorophores, which makes them easy to detect. For spherical compounds, diffusion coefficients D can be calculated by the Stokes–Einstein equation:

$$D = \frac{kT}{6\pi\eta R} \quad (7)$$

where η is the solvent viscosity at temperature T, k the Boltzman constant, and R the Stokes radius of the chromophore.

Figure 3 presents a typical fluorescence correlation curve obtained for fluorescent latex beads in suspension in water at room temperature (T = 295 K). The best adjustment between experimental data and the theoretical curve results in a translational diffusion time of 2.2 ms. Taking into account this τ_D value and that of the diffusion constant of beads in water, $D_w = 1.6 \times 10^{-7}$ cm^2/s (obtained for a water viscosity at room temperature η_w = 0.96 cp at 295 K and a latex bead radius R = 14 nm), a beam-waist value of 0.54 μm was thus obtained according to Eq. (5). This parameter, which is used in the diffusion coefficient determination, requires great accuracy. This can be reached by determination of the translational diffusion time (τ_D) as a function of the viscosity (η) of the solution. Indeed, from Eqs. (4) and (7), τ_D values can be expressed as a function η as follows:

$$\tau_D = \frac{\omega_0^2}{8D_w \eta_w} \eta \quad (7)$$

where D_w is the diffusion coefficient of the fluorophore in water and η_w the water viscosity.

Curves obtained for latex beads and FITC–dextran of molecular weight 40 and 150 kDa are shown in Figs. 4a–c. Similar beam-waist values were found for the three species. Taking the mean value $\omega_0 = 0.50 \pm 0.04$ μm, the focal depth was thus $z_0 = 1.7 \pm 0.2$ μm, corresponding to an excitation volume of about 3 μm^3.

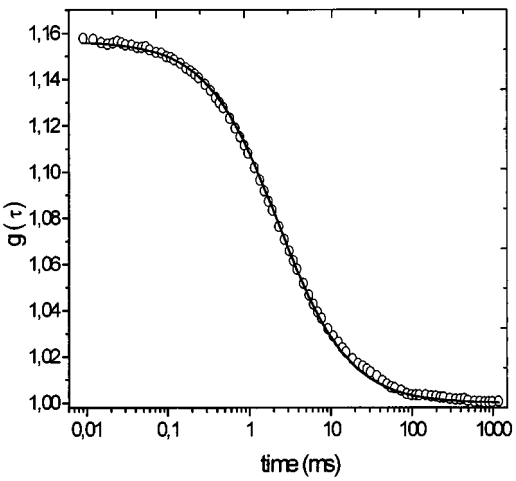

Fig. 3. Experimental $g(\tau)$ (○) and theoretical curve (——) for 28-nm-diameter fluorescent beads in water. Sampling time during acquisition was 10 μs. Parameters obtained by fit are τ_d = 2.2 ms and ω_0/z_0 = 0.3.

Fluorescence Intensity Autocorrelation

Diffusion Coefficient of FITC–Dextran by TPE: Comparison with FRAP Results

Fluorescence correlation functions for FITC–dextran of four molecular weights were studied. Figure 5 presents a typical curve obtained for a 40-kDa FITC–dextran solution. Values of τ_D obtained from the fitting of experimental curves and corresponding diffusion constants D_{exp} calculated from Eq. (4) are summarized in Table II. The linear relationship between τ_D and the Stokes radius of each FITC–dextran molecule is verified (Fig. 5, inset). Previous determination of FITC–dextran diffusion coefficients by the fluorescence recovery after photobleaching method (FRAP) [18] are also reported in Table I. Concordant results are obtained by both FRAP and FCM with TPE, despite the great differences in the experimental conditions.

TPE of GFP Solutions

Wild GFP and different mutants have attracted considerable interest for their specific spectroscopic proper-

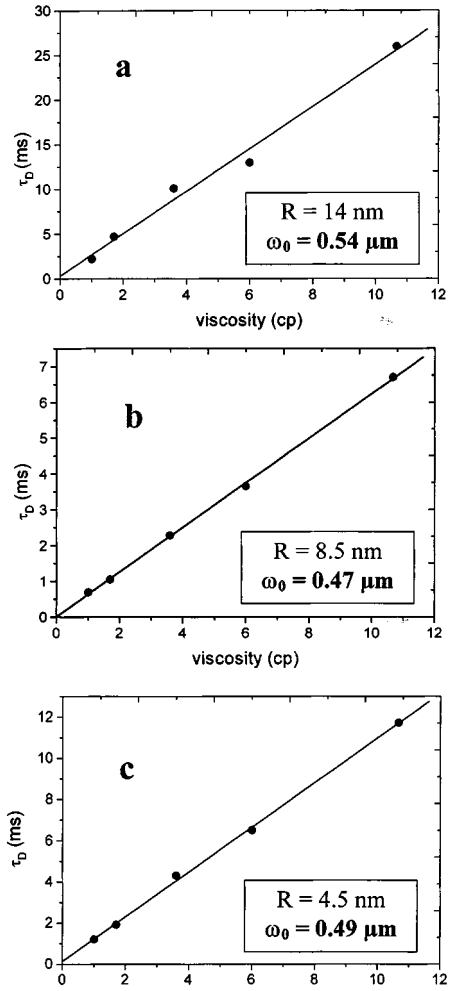

Fig. 4. Variation of the diffusion time τ_d with the viscosity on the sample: (a) 28-nm-diameter fluorescent beads; (b) 150-kDa FITC–dextran; (c) 40-kDa FITC–dextran. *R* corresponds to the Stokes radius of the chromophore, and ω_0 to the beam-waist value.

ties, making them interesting fluorophores for investigating cellular systems. For example, rGFP, rGFPuv, and rEGFP have very different one-photon absorption properties. The absorption spectrum of rGFP presents two maxima, which have been attributed to two protonation states of the chromophore [19,20]. The first maximum, at 392 nm, is attributed to the neutral form (A), while the second one, at 475 nm, is attributed to the anionic state (B). In the case of rGFPuv at pH 8, only the neutral form A is present, while rEGFP exists only in the anionic form B [21].

Although the emission fluorescence spectra of chromophore remain basically the same for one-photon excitation (OPE) and TPE, the absorption spectra can differ [22], and it is hardly possible to predict TPE wavelength maxima. For this purpose, we have undertaken the TPE

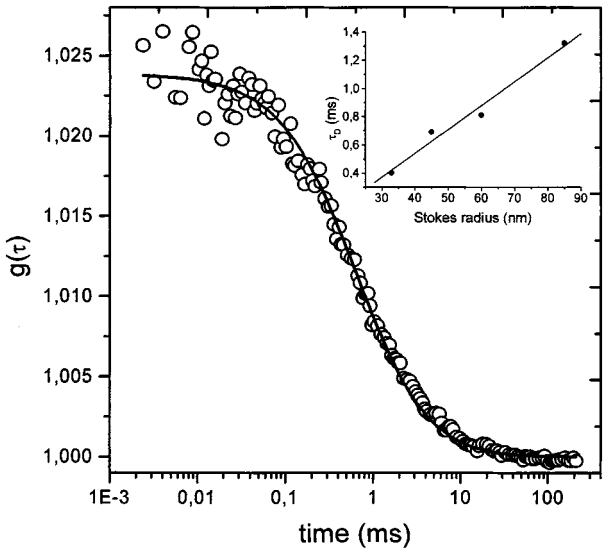

Fig. 5. Experimental $g(\tau)$ (○) and theoretical curve (——) for 40-kDa FITC–dextran in 5 m*M* HEPES buffer, pH 7.5. Sampling time during acquisition was 0.8 μs. The diffusion time obtained by fit is $\tau_d = 0.69$ ms.

excitation of rGFP, rGFPuv, and rEGFP. The relative fluorescence intensity for the three molecular species obtained under two-photon oxcitation is given in Table II for two excitation intensities. Results show that two-photon absorption cross sections of rGFP and rGFPuv allow significant excitation at 800 nm, while for rEGFP, TPE is negligible at this wavelength, showing a concordance between one- and two-photon absorption properties for these molecules.

For the first time, diffusion coefficient measurements of rGFP and rGFPuv have been undertaken with FCM under TPE. A typical rGFP fluorescence correlation curve is presented in Fig. 6. The fit of experimental points reveals a contribution from a reversible nonfluorescent state with a lifetime estimated as 6 μs. This fast compo-

Table I. Diffusion Constants of FITC–Dextran in Aqueous Solutions[a]

FITC–dextran	*R* (nm)	τ_D (ms)	D_{exp} (μm^2/s)	D_0 (μm^2/s)	D_{FRAP} (μm^2/s)
20,000 Da	3.3	0.40	78	68	64 ± 2
40,000 Da	4.5	0.69	45	49	44 ± 5
70,000 Da	6	0.81	38	37	30 ± 2
150,000 Da	8.5	1.3	24	26	26 ± 2

[a] Stokes radii *R* for the different molecular weights are from the Sigma product information sheet. Theoretical diffusion coefficients D_0 are calculated from the Stokes–Einstein equation (7). Experimental diffusion coefficients D_{exp} obtained by fluorescence correlation microscopy are compared with results obtained by the FRAP method.

Table II. Relative Fluorescence Intensity of rGFPuv, rGFP, and rEGFP Excited at 800 nm by Two-Photon Absorption[a]

	Relative fluorescence intensity	
Excitation intensity	2.3×10^{30} photons cm^{-2} s^{-1}	3×10^{29} photons cm^{-2} s^{-1}
rGFPuv	1	1
rGFP	0.87	0.87
rEGFP	0.09	0.05

[a] The results are shown for two excitation intensities. Protein concentration in 5 m*M* Tris buffer, pH 8: 80 n*M*.

nent, previously observed in confocal one-photon excitation experiments, was attributed to a proton transfer reaction in the fundamental state [21–23]. A similar fluorescence correlation curve was obtained with rGFPuv. A diffusion coefficient of 8.3×10^{-7} cm^2/s was found for the two GFP species. This result is in good agreement with the previously reported value of $D = 8.7 \times 10^{-7}$ cm^2/s obtained with FCM under confocal one-photon excitation [19] and the FRAP method [24].

Single-Molecule Detection of Fluorescein

Fluorescein is also of particular interest for intracellular applications like pH measurements. One difficulty in studying such dyes by FCM is their very small size (MW, 330 Da). These molecules diffuse through the excitation volume more quickly compare to dextran or GFP and thus the fluorescence signal emitted during the counting interval by a single fluorophore is weaker.

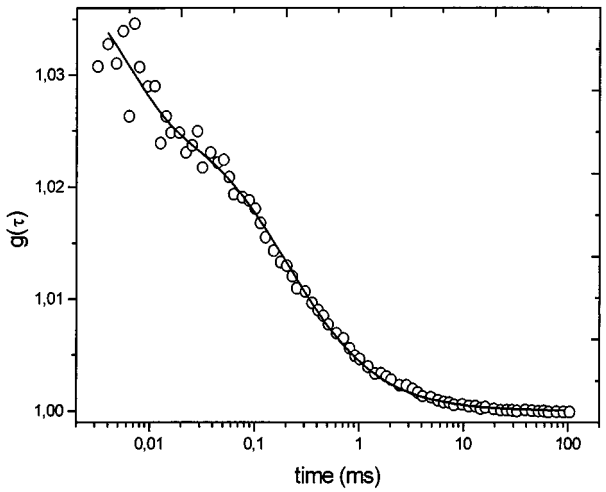

Fig. 6. Experimental $g(\tau)$ (○) and theoretical curve (——) for rGFP in 5 m*M* Tris buffer, pH 8. Sampling time during acquisition was 0.8 μs. Best-fit parameters are $\tau_d = 0.38$ ms and $\tau_T \sim 6$ μs.

FCM measurement of fluorescein under TPE has been carried out taking advantage of its high two-photon absorption cross section at 800 nm [16,17]. The fluorescence correlation curve for 800 p*M* fluorescein at physiological pH is presented in Fig. 7. Under these conditions, single-molecule detection was reached since the average number of molecules in the excitation volume was less than one ($N = 0.8$ molecule). The rapid decay (lifetime, ~ 2 μs) corresponds to a proton transfer reaction between fluorescein and the solvent [25]. The diffusion coefficient of fluorescein calculated from experimental data was 300 $\mu m^2/s$, a value in good agreement with the result obtained by FCM with OPE [15].

CONCLUSION

Square-law dependence of fluorescence intensity with respect to excitation intensity was checked over a large intensity domain for FITC–dextran, GFP, and fluorescein. A rigorous calibration of the excitation volume was made to obtain very accurate values of the excitation volume dimensions. Two-photon excitation FCM was successfully applied to the study of diffusion coefficients of the three molecular probes, and, in the case of fluorescein, our experimental setup was applied to single-molecule detection. The present results offer good perspectives in the study of these molecular probes in two-photon excitation FCM of living cells.

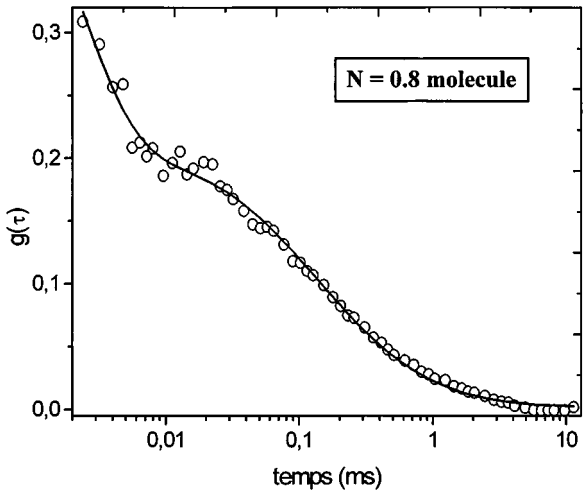

Fig. 7. Detection of a single molecule of fluorescein: Experimental $g(\tau)$ (○) and theoretical curve (——) for fluorescein, 800 p*M*, in HEPES buffer, pH 7.5. Sampling time during acquisition was 0.8 μs. Parameters obtained by fit are $N = 0.8$, $\tau_d = 0.11$ ms, and $\tau_T \sim 2$ μs.

REFERENCES

1. E. L. Elson and D. Madge (1974) *Biopolymers* **13**, 1–27.
2. S. R. Aragon and R. Pecora (1976) *J. Chem. Phys.* **64**, 1791–1803.
3. M. Ehrenberg and R. Rigler (1974) *Chem. Phys.* **4**, 390–401.
4. S. Weiss (1999) *Science* **283**, 1676–1683.
5. R. Brock, M. A. Hink, and T. Jovin (1998) *Biophys. J.* **75**, 2547–2557.
6. J. Widengren and R. Rigler (1998) *Cell. Mol. Biol.* **44**, 857–879.
7. H. Quian and E. L. Elson (1991) *Appl. Opt.* **30**, 1185–1195.
8. R. Rigler, U. Mets, J. Widengren, and P. Kask (1993) *Eur. Biophys. J.* **22**, 169–175.
9. J. R. Fries, L. Brand, C. Eggeling, M. Köllner, and C. A. M. Seidel (1998) *J. Phys. Chem. A* **102**, 6601–6613.
10. K. M. Berland, P. T. C. So, and E. Gratton (1995) *Biophys. J.* **68**, 694–701.
11. J. Mertz, C. Xu, and W. W. Webb (1995) *Opt. Lett.* **20**, 2532–2534.
12. P. Shcwille, U. Haupts, S. Maiti, and W. W. Webb (1999) *Biophys. J.* **77**, 2251–2265.
13. L. Brand, C. Eggeling, C. Zander, K. H. Drexhage, and C. A. M. Seidel (1997) *J. Phys. Chem. A* **101**, 4313–4321.
14. D. E. Koppel (1974) *Phys. Rev. A* **10**, 1938–1945.
15. Y. Chen, J. D. Müller, K. M. Berland, and E. Gratton (1999) *Methods* **19**, 234–252.
16. Fisher, C. Cremer, and E. H. K. Stelzer (1995) *Appl. Opt.* **34**, 1989–2003.
17. C. Xu and W. W. Webb (1996) *J. Opt. Soc. Am. B* **13**, 481–491.
18. M. Arrio-Dupont, S. Cribier, G. Foucault, P. F. Devaux, and A. d'Albis (1996) *Biophys. J.* **70**, 2327–2332.
19. B. R. Terry, E. K. Matthews, and J. Haseloff (1995) *Biochem. Biophys. Res. Commun.* **217**, 21–27.
20. G. Jung, J. Wiehler, W. Göhde, J. Tittel, Th. Basché, B. Steipe, and C. Bräuchle (1998) *Bioimaging* **6**, 54–61.
21. U. Haupts, S. Maiti, P. Scwhille, and W. W. Webb (1998) *Proc. Natl. Acad. Sci. USA* **95**, 13573–13578.
22. C. Xu, W. Zipfel, J. B. Shear, R. M. Williams, and W. W. Webb (1996) *Proc. Natl. Acad. Sci. USA* **93**, 10763–10768.
23. M. Chattoraj, B. A. King, G. U. Bublitz, and S. G. Boxer (1996) *Proc. Natl. Acad. Sci. USA* **93**, 8362–8367.
24. R. Swaminathan, C. P. Hoang, and A. S. Verkman (1997) *Biophys. J.* **72**, 1900–1907; *Biophys. J.* **70**, 2327–2332.
25. M. M. Martin and L. Lindqvist (1975) *J. Luminesc.* **10**, 381–390.